Inorganica Chimica Acta 362 (2009) 1348–1354

Contents lists available at ScienceDirect

Inorganica Chimica Acta

journal homepage: www.elsevier.com/locate/ica

Iron and cobalt complexes of 2,6-diacetylpyridine-bis(R-thiosemicarbazone) (R = H, phenyl) showing unprecedented ligand deviation from planarity

Anangamohan Panja [a], Charles Campana [b], Christopher Leavitt [a], Michael J. Van Stipdonk [a], David M. Eichhorn [a,*]

[a] Department of Chemistry, Wichita State University, Wichita, KS 67260, USA
[b] Bruker-AXS, Madison, WI, USA

ARTICLE INFO

Article history:
Received 1 February 2008
Received in revised form 23 June 2008
Accepted 24 June 2008
Available online 3 July 2008

Keywords:
Iron complexes
Cobalt complexes
X-ray crystal structures
Nitrile hydratase

ABSTRACT

The syntheses, characterization, and single-crystal X-ray crystal structures are reported for four complexes of iron and cobalt with the pentadentate ligands, 2,6-diacetylpyridinebis(thiosemicarbazone) (H_2L^1) and 2,6-diacetylpyridinebis(phenylthiosemicarbazone) (H_2L^2), including a cobalt dimer displaying a deviation from planarity which is unprecedented for this class of ligands and allows the ligand to occupy five positions of a pseudo-octahedral coordination sphere. This dimer reacts with KCN to produce a mononuclear complex of relevance to the active site of cobalt nitrile hydratase.

1. Introduction

Thiosemicarbazone ligands, derived from the combination of a thiosemicarbazide and an aldehyde or ketone, are a useful ligand type for obtaining coordination spheres with mixed N/S donors. Interest in these ligands has been driven, in part, by p'otentially beneficial biological activity of the ligands and their metal complexes, including antitumor [1], fungicidal [2], bactericidal [3], and antiviral [4] activity. Our continued interest in synthesizing model complexes for the active sites of metalloenzymes with mixed N/S coordination spheres [5], such as nitrile hydratase [6] and the A-cluster of carbon monoxide dehydrogenase/acetyl coenzyme A synthase [7], has led us to investigate metal complexes of this class of ligands.

Coordination of the thiosemicarbazone ligand is generally through the azomethine N atom and the S atom. The ligand can bind either as the neutral species or monodeprotonated (Fig. 1). Crystallographically, this difference can generally be monitored by the length of the C–S bond; the neutral ligand contains a formal C–S double bond with bond lengths on the order of 1.67–1.72 Å while the deprotonated ligand undergoes tautomerization to produce a formal C–S single bond with bond lengths on the order of 1.71–1.80 Å [8].

With an eye on synthesizing model complexes for the active site of the nitrile hydratase enzymes, which have a N_2S_3 donor set [9], we have focused on Fe and Co complexes of pentadentate bis(thiosemicarbazone) ligands synthesized by the condensation of two equivalents of a thiosemicarbazide with a dialdehyde or diketone bearing a potential coordinating atom. In particular, we have employed thiofuran-2,5-dicarboxaldehyde and 2,6-diacetylpyridine – complexes of ligands derived from the latter are described herein. Although not as intensely studied as the monothiosemicarbazones, the bis(thiosemicarbazones) have been the subject of a number of investigations, with some indication of biological activity on the part of these ligands and their metal complexes [10]. A search of the Cambridge Crystallographic Database [8] for transition metal complexes of bis(thiosemicarbazone) ligands derived from 2,6-diacetylpyridine yields 13 structures including mononuclear [3a,11], dinuclear [11a,11d,12], and tetranuclear [12c] species and a total of seven different structural types (Fig. 2), indicating the coordinative flexibility of this class of ligands. We have found that the isolated crystalline material is highly dependent on the semicarbazide substituent and the metal salt used to synthesize the complex.

2. Experimental

2.1. General

Unless otherwise stated, all solvents and reagents were used as received from Aldrich, Acros, and Fisher Scientific without further

---

* Corresponding author. Tel.: +1 316 978 7367; fax: +1 316 978 3431.
E-mail address: david.eichhorn@wichita.edu (D.M. Eichhorn).

0020-1693/$ - see front matter
doi:10.1016/j.ica.2008.06.031

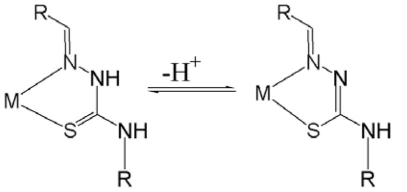

Fig. 1. Thiosemicarbazone ligands showing the common bonding modes of the neutral and anionic ligand.

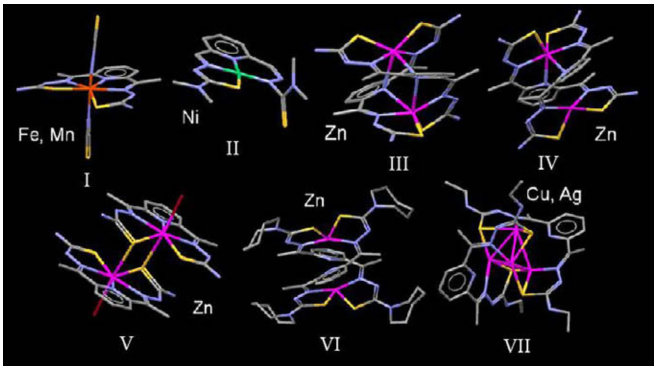

Fig. 2. Mercury drawings downloaded from the Cambridge Crystallographic Database [8] for structures from references [11a,11c,11e] and [12a–c] representing the seven structural types in the literature for 2,6-diacetylpyridinebis(thiosemicarbazone) complexes and indicating the metals for which structures have been reported.

purification. 2,6-Diacetylpyridinebis(thiosemicarbazone) [10] (H_2L^1) and 2,6-diacetylpyridinebis(phenylthiosemicarbazone) [13] (H_2L^2) were synthesized as previously described. IR spectra were recorded on a Nicolet Avatar 360 FTIR. Electrochemical characterization was performed in acetonitrile with [NEt_4ClO_4] as supporting electrolyte using a PAR 263A potentiostat/galvanostat with a Pt disk working electrode and a Ag/AgCl reference electrode. Potentials are quoted with respect to Ag/AgCl. UV/Visible spectra were obtained using a Hitachi U-2010 spectometer. Mass spectra were obtained on a Varian 1200 LC/MS using ESI ionization technique. Conductivity measurements were made with a Systronics (India) direct reading conductivity meter (model 304) and magnetic susceptibility measurements were carried out on a PAR 155 vibrating sample magnetometer. The data were corrected for diamagnetic susceptibilities using Pascal's constants. Elemental analyses were obtained from M-H-W Laboratories, Phoenix, AZ.

*2.2. 2,6-Diacetylpyridinebis(thiosemicarbazone)dichloro iron(III) chloride [$H_2L^1FeCl_2$]Cl (**1**)*

In 50 mL of methanol were combined 155 mg (0.50 mmol) of H_2L^1 and 135 mg (0.50 mmol) of $FeCl_3 \cdot 2.5H_2O$ The mixture was heated at reflux for 1 h, resulting in a greenish-brown crystalline precipitate which was isolated and washed with methanol and diethyl ether to give 215 mg (0.41 mmol, 82%) of **1** as a greenish-brown crystalline material. X-ray quality crystals were grown by slow evaporation of a methanol solution. IR (KBr pellet, cm^{-1}): 3314s, 3255s, 3127s, 2907m, 1602vs, 1552vs, 1464m, 1403m, 1366m, 1191s, 1107m, 815w, 799w, 599w. *Elem. Anal. Calc.* for $C_{11}H_{15}N_7FeCl_3 \cdot 3H_2O$: C, 25.14; H, 4.03; N, 18.66. Found: C, 25.00; H, 3.87; N, 18.70%. E-chem: irr. wave at −960 mV. UV–Vis, nm (ε): 238 (262 800), 319 (67 700), 718 (246). Mass Spec. (positive mode): 363 $[M–2HCl]^+$.

*2.3. 2,6-Diacetylpyridinebis(phenylthiosemicarbazone)(chloro)-(methanol)iron(II) chloride [$H_2L^2Fe(MeOH)(Cl)$]Cl (**2**)*

Under a nitrogen atmosphere, 115 mg (0.25 mmol) of 2,6-diacetylpyridinebis(phenylthiosemicarbazone) and 41 mg (0.25 mmol) of anhydrous $FeCl_3$ were combined in 40 mL of dry methanol to give a green solution. The volume was reduced to 10 mL and upon standing at room temperature gave a green microcrystalline precipitate of **2** (108 mg, 0.175 mmol, 70%). X-ray quality crystals were grown by slow evaporation of a solution in 50/50 methanol/acetonitrile. *Elem. Anal. Calc.* for $C_{24}H_{27}N_7S_2Cl_2OFe$: C, 46.47; H, 4.39; N, 15.81. Found: C, 46.28; H, 4.12; N, 16.00%. E-chem: $E_{1/2}$ = 75 mV ($E_p^c - E_p^a = 210$ mV), irr. waves at 1000 mV, −1270 mV. UV–Vis, nm (ε): 252 (70 500), 343 (45 200), 753 (sh, 400). Mass Spec. (positive mode): 585/587 (M^+).

*2.4. Bis(2-acetylphenylthiosemicarbazone-6-acetylpyridine)iron(III) perchlorate [$(L^{2'})_2Fe$]ClO_4 (**3**)*

To 60 mL of methanol was added 230 mg (0.50 mmol) of 2,6-diacetylpyridinebis(phenylthiosemicarbazone) and 230 mg (0.50 mmol) of $Fe(ClO_4)_3$, giving rise to a brown precipitate which was washed with methanol and diethyl ether to give 300 mg (0.30 mmol, 60%) of **3** as a brown powder. X-ray quality crystals were grown by slow cooling of a DMF solution. IR (KBr pellet, cm^{-1}): 3420br, 3079w, 1713m, 1598m, 1549m, 1507vs, 1458m, 1441s, 1399m, 1364m, 1318m, 1192w, 1158m, 1115s, 810m, 747m, 691m, 622m, 584w, 505w. *Elem. Anal. Calc.* for $(C_{32}H_{30}N_8O_2Fe)ClO_4 \cdot H_2O$: C, 48.29; H, 4.05; N, 14.08. Found: C, 47.75; H, 3.89; N, 14.30%. E-chem: $E_{1/2}$ = 0.0 mV ($E_p^c - E_p^a = 78$ mV). UV–Vis, nm (ε): 226 (246 500), 390 (30 600), 669 (240), 850 (sh, 220). Mass spec.: 678 (M^+).

*2.5. Bis[2,6-diacetylpyridinebis(thiosemicarbazone)(acetonitrile)cobalt(II)] perchlorate [$H_2L^1Co(CH_3CN)]_2(ClO_4)_4$ (**4**)*

To 50 mL of methanol was added 155 mg (0.50 mmol) of 2,6-diacetylpyridinebis(thiosemicarbazone) and 180 mg (0.50 mmol) of $Co(ClO_4)_2$. The mixture was heated for 1 h, giving rise to a brownish-orange solution. The resulting mixture was reduced to 10 mL and upon sitting at room temperature, 210 mg (0.175 mmol, 70%) of **4** was isolated as a dark orange crystalline material. X-ray quality crystals were grown by slow evaporation of a solution in acetonitrile/methanol. IR (KBr pellet, cm^{-1}): 3417br, 1617s, 1558m, 1472w, 1384w, 1307w, 1274w, 1193m, 1121vs, 1108vs, 1083vs, 1031s, 625s, 521s. *Elem. Anal. Calc.* for $(C_{26}H_{36}N_{16}S_4Co_2)(ClO_4)_4$: C, 25.67; H, 2.98; N, 18.42. Found: C, 26.17; H, 3.35; N, 17.60%. E-chem: irr. waves at −580 mV and −1440 mV. UV–Vis, nm (ε): 320 (43 500), 447 (sh, 13 000). Mass spec. (positive mode): multiplets at 1113 $[M(ClO_4)_3]^+$, 1073 $[(M–CH_3CN)(ClO_4)_3]^+$, 1032 $[(M–2CH_3CN)(ClO_4)_3]^+$, 466.5 $[(M–2CH_3CN)(ClO_4)_2]^{2+}$.

*2.6. Bis[2,6-diacetylpyridinebis(phenylthiosemicarbazone) cobalt(III)] nitrate [$L^2Co]_2(NO_3)_2$ (**5**)*

To 50 mL of methanol were added 230 mg (0.50 mmol) of 2,6-diacetylpyridinebis(phenylthiosemicarbazone) and 150 mg (0.50 mmol) of $Co(NO_3)_2$. The mixture was heated at reflux for 1 h and reduction of the volume to 10 mL gave 255 mg (0.21 mmol, 84%) of **5** as a brown powder. X-ray quality crystals were grown by slow evaporation of a solution in 50/50 methanol/acetonitrile. IR (KBr pellet, cm^{-1}): 3425br, 1652m, 1616m, 1581m, 1539s, 1496m, 1441m, 1384vs, 1318m, 1253m, 1194m, 1155m, 1120m, 811w, 753m, 691m, 578w, 498w. *Elem. Anal. Calc.* for $(C_{46}H_{42}N_{14}S_4Co_2)(NO_3)_2 \cdot 2H_2O$: C, 46.16; H, 3.87; N, 18.72. Found: C, 46.35; H, 3.65; N, 19.00%. E-chem: irr. wave at −800 mV. UV–Vis, nm (ε): 388 (32 700), 257 (74 000), 205 (134 800). Mass spec. (positive mode): 1035 [M–H]$^+$.

2.7. *(2,6-Diacetylpyridinebis(phenylthiosemicarbazone))cyanocobalt(III) [$L^2Co(CN)$] (**6**)*

To 40 mL of methanol were added 150 mg (0.125 mmol) of **5** and 20 mg (0.25 mmol) of KCN. The mixture was stirred overnight and the solvent was removed. The resulting brown solid was washed with water and dried to yield 110 mg (0.19 mmol, 78%) of **6** as a brown solid. IR (KBr pellet, cm^{-1}): 3470br, 3068w, 2122m, 1598s, 1495vs, 1460s, 1439vs, 1402s, 1371m, 1318m, 1253m, 1160m, 1090m, 807w, 753m, 692m, 503w. *Elem. Anal. Calc.* for $C_{24}H_{21}N_8S_2Co \cdot H_2O$: C, 51.25; H, 4.12; N, 19.92. Found: C, 51.28; H, 3.60; N, 19.82%. E-chem: irr. wave at −1130 mV. UV–Vis, nm (ε): 207 (137 000), 260 (133 000), 381 (57 000). Mass spec. (positive mode): 518 [M–CN]$^+$.

2.8. *X-ray crystallography*

Data for **1** were collected using a Bruker APEX diffractometer (Cu Kα, λ = 1.54178 Å) equipped with Bruker KRYO-FLEX low-temperature apparatus. Data for **2**–**5** were collected using a Bruker Kappa APEXII diffractometer (Mo Kα, λ = 0.71069 Å) equipped with an Oxford Cryosystems Cryostream 700 low-temperature apparatus. Suitable crystals were identified under a polarizing microscope and affixed with oil in a Hampton Research Cryoloop and transferred to the coldstream of the diffractometer. Data reduction was performed using Bruker SAINT [14] software, structure solution (direct methods) and refinement (full-matrix least-squares) using SHELXS-97 and SHELXL-97 [15] within the Bruker SHELXTL suite. Data were corrected for Lorentz and polarization effects and for absorption using the Bruker SADABS [14] program (multiscan for **1**, face indexing for **2**–**5**). Hydrogen atoms were placed at calculated idealized positions and were not refined. All non-hydrogen atoms were refined using anisotropic thermal parameters. Pertinent details are given in Table 1.

3. Results and discussion

Two ligands were employed in this study, both derived from the condensation of two equivalents of a thiosemicarbazide with 2,6-diacetyl pyridine – L^1 employs unsubstituted thiosemicarbazide and L^2 has a phenyl group substituted on the terminal N atoms.

3.1. *Iron chemistry*

Using the unsubstituted ligand and $FeCl_3$, we isolated the mononuclear Fe(III) complex [$H_2L^1FeCl_2$]Cl (**1**). Room temperature magnetic susceptibility and conductivity measurements (Table 4) are consistent with this formulation. An ORTEP drawing of the cation in **1** is shown in Fig. 3, with data collection and structure solution parameters in Table 1 and selected bond distances and angles in Tables 2 and 3. The complex sits on a general position in the orthorhombic space group Pbca and crystallizes with three water molecules in the asymmetric unit. The structure is of type **I**, with pentagonal bipyramidal coordination around the Fe(III); the five donor atoms of the essentially planar ligand comprise the equatorial pentagonal plane and two chloride ligands are in the axial positions. The chloride counterion is involved in a hydrogen bond with

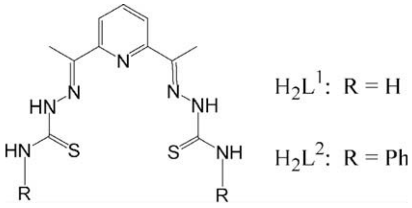

Table 1

X-ray data collection and structure solution parameters for **1**–**5**

	1	**2**	**3**	**4**	**5**
Formula	$C_{11}H_{21}N_7O_3S_2Cl_3Fe$	$C_{24}H_{27}N_7OS_2Cl_2Fe$	$C_{41}H_{51}N_{11}O_9S_2ClFe$	$C_{26}H_{36}N_{16}Cl_4Co_2O_{16}S_4$	$C_{46}H_{46}N_{16}Co_2O_8S_4$
Mol. wt.	525.67	620.40	997.34	1216.60	1197.07
Color	brown	green	dark	dark orange	dark red
Habit	block	block	block	block	block
Temperature (K)	100	150	150	150	150
Diffractometer	Bruker APEX	Bruker K-APEXII	Bruker K-APEXII	Bruker K-APEXII	Bruker K-APEXII
Crystal System	orthorhombic	monoclinic	monoclinic	triclinic	monoclinic
Radiation	Cu Kα	Mo Kα	Mo Kα	Mo Kα	Mo Kα
Space group	*Pbca*	$P2_1/n$	$P2/c$	$P\bar{1}$	$C2/c$
a (Å)	12.6799(4)	13.146(5)	14.545(5)	8.588(5)	25.241(5)
b (Å)	14.2998(5)	11.186(5)	10.644(5)	12.079(5)	16.298(5)
c (Å)	22.3519(7)	19.496(5)	14.951(5)	12.741(5)	13.478(5)
α (°)	90	90	90	62.893(5)	90
β (°)	90	108.910(5)	94.010(5)	71.769(5)	112.246(5)
γ (°)	90	90	90	81.909(5)	90
V (Å^3)	4052.8(2)	2712.2(17)	2309.0(16)	1117.4(9)	5132(3)
Z	8	4	2	1	2
D_{calc} (g cm^{-3})	1.723	1.519	1.434	1.808	1.544
μ (mm^{-1})	11.801	0. 940	0.540	1.254	0.879
$F(000)$	2152	1280	1024	618	2448
Dimension (mm)	.09 × .09 × .02	0.18 × 0.30 × 0.38	.20 × .20 × .20	.30 × .28 × .18	.38 × .20 × .10
θ Range (°)	3.96–63.76	1.65–26.72	1.40–26.54	1.87–27.14	1.52–23.64
Reflections/unique (R_{iint})	35 986/3144 (0.0428)	52 125/5747 (0.0590)	37 759/4752 (0.0957)	45 929/4874 (0.0615)	36 047/3828 (0.1090)
>2$\sigma(I)$/parameters	2520/263	4202/353	3460/305	3433/360	2396/345
Completeness to θ_{max}	93.9	99.8	98.5	98.5	99.2
Goodness-of-fit	1.028	1.099	1.065	0.953	1.035
R_1/wR_2 ($I > 2\sigma(I)$)	0.0389/0.0980	0.0401/0.1039	0.0592/0.1778	0.0580/0.1651	0.0538/0.1302
R_1/wR_2 (all)	0.0535/0.1072	0.0626/0.1182	0.0811/0.1913	0.0897/0.1915	0.1095/0.1684
Ext. Coefficient	none	none	0.0012(10)	none	none
Peak/hole (eÅ^{-3})	0.951/−0.337	0.472/−0.348	0.650/−0.457	1.145/−0.990	0.557/−0.653

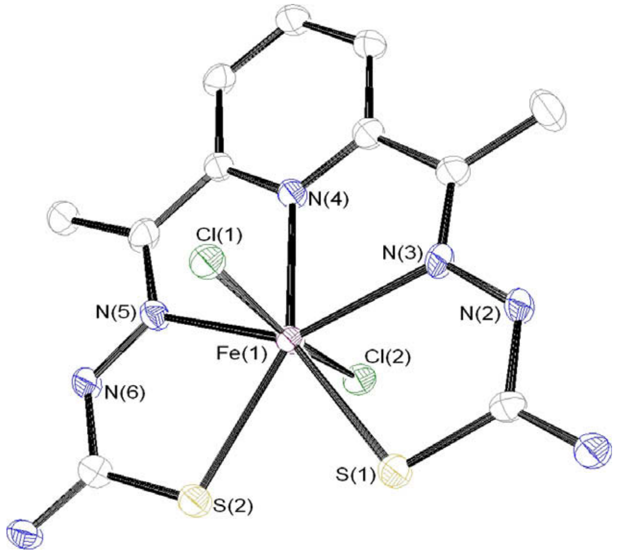

Fig. 3. ORTEP drawing of the cation in **1**, showing 50% ellipsoids. H atoms omitted for clarity.

one terminal amine (Cl3···N7 3.240 Å). A hydrogen bonding network involving all three water molecules links the Fe-containing cations together. Bond lengths are within the normal range for Fe(III) and the Fe–S bonds (2.494 and 2.529 Å) and C–S bonds (1.685 and 1.687 Å) are consistent with a neutral ligand containing C–S double bonds.

The structure of **1** is similar to others that have been reported for mononuclear complexes of divalent transition metal ions, including Zn [11a], Fe [11c], and Mn [11b,11d]. The Zn, Fe, and one of the Mn structures are entirely analogous to that of **1**, with a neutral unsubstituted ligand and two anionic ligands in the axial positions, while the structure of $[LMn(EtOH)_2]$ has the ligand doubly deprotonated with two neutral ethanol ligands in the axial positions. Interestingly, in the mass spectrum, the only detectable ion corresponds to a loss of two molecules of HCl, i.e., double deprotonation of the ligand to produce the $[L^1Fe]^+$ ion. The extent of planarity of the ligand can be defined by the dihedral angles between two planes: (i) the plane of the three coordinated N atoms and (ii) the plane containing the metal, a coordinated S atom, and the coordinated N atom nearest to it. All of the previous structures, along with that of **1**, feature relatively planar ligands, with dihedral angles ranging from 0.72° to 11.30°. In **1**, these dihedral angles are both equal to 1.00° giving the most planar ligand of all reported complexes of this type.

When the phenyl-substituted ligand $\mathbf{L^2}$ was employed, a mononuclear complex was also isolated, but crystallographic characterization (confirmed by elemental analysis) unexpectedly identified it as an Fe(II) complex, although the reductant has not been identified. It should be noted that $[H_2L^1Fe^{II}(SCN)_2]$ was also prepared by reaction of H_2L^1 with $FeCl_3$ [11c]. An ORTEP drawing of $[H_2L^2Fe(MeOH)(Cl)]Cl$ (**2**) is shown in Fig. 4, with data collection and structure solution parameters in Table 1 and selected bond distances and angles in Tables 2 and 3. Also displaying type **I**, the molecule sits on a general position in the monoclinic space group $P2_1/n$ with the methanol ligand engaging in hydrogen bonding with the chloride counterion (Cl2···O1 3.104 Å). Both the coordinated and noncoordinated Cl's also form hydrogen bonds with the two N atoms bound to the C–S moiety, giving rise to a chain of Fe molecules held together by hydrogen bonding. Bond lengths are within the normal range for Fe(II) and the Fe–S bonds (2.581 and 2.668 Å) and C–S

Table 2
Selected bond distances (Å) for **1**–**5**

	1		**2**		**3**	
M–S bonds	Fe(1)–S(1)	2.5292(10)	Fe(1)–S(1)	2.5806(11)	Fe(1)–S(1)	2.2025(12)
	Fe(1)–S(2)	2.4934(10)	Fe(1)–S(2)	2.6678(9)		
$M–N_{py}$ bonds	Fe(1)–N(4)	2.184(3)	Fe(1)–N(4)	2.224(2)	Fe(1)–N(2)	1.925(3)
$M–N_{axo}$ bonds	Fe(1)–N(5)	2.254(3)	Fe(1)–N(3)	2.286(2)	Fe(1)–N(1)	2.036(3)
	Fe(1)–N(3)	2.295(3)	Fe(1)–N(5)	2.310(2)		
	4		**5**			
M–S bonds	Co(1)–S(2)	2.525(2)	Co(1)–S(1)	2.292(2)		
	Co(1)–S(1)	2.592(2)	Co(1)–S(2)	2.227(2)		
	Co(1)–S(1′)	2.629(2)	Co(1)–S(2′)	2.300(2)		
$M–N_{py}$ bonds	Co(1)–N(4)	2.160(3)	Co(1)–N(4)	1.845(4)		
$M–N_{axo}$ bonds	Co(1)–N(5)	2.253(4)	Co(1)–N(3)	1.903(4)		
	Co(1)–N(3)	2.278(4)	Co(1)–N(5)	1.887(4)		

Table 3
Selected bond angles (°) for **1**–**5**

1		**2**		**3**	
N(4)–Fe(1)–N(3)	70.43(10)	N(4)–Fe(1)–N(3)	69.79(8)	N(2)–Fe(1)–N(1)	79.95(11)
N(4)–Fe(1)–S(1)	144.00(8)	N(4)–Fe(1)–S(1)	144.02(6)	N(2)–Fe(1)–S(1)	84.91(9)
N(3)–Fe(1)–S(1)	73.59(7)	N(3)–Fe(1)–S(1)	74.25(6)	N(1)–Fe(1)–S(1)	163.16(8)
S(2)–Fe(1)–S(1)	70.47(3)	S(1)–Fe(1)–S(2)	75.21(3)	N(1′)–Fe(1)–S(1)	91.10(9)
Cl(1)–Fe(1)–Cl(2)	168.09(4)	O(1)–Fe(1)–Cl(1)	174.78(5)	N(2′)–Fe(1)–S(1)	87.94(9)
				S(1′)–Fe(1)–S(1)	95.70(6)
4		**5**			
N(4)–Co(1)–N(3)	70.65(14)	N(4)–Co(1)–N(5)	82.28(18)	N(4)–Co(1)–S(1)	103.71(15)
N(4)–Co(1)–S(1)	141.70(11)	N(4)–Co(1)–N(3)	80.90(18)	N(5)–Co(1)–S(1)	103.29(14)
N(3)–Co(1)–S(2)	142.98(11)	N(5)–Co(1)–S(2)	86.07(13)	N(3)–Co(1)–S(1)	75.85(15)
S(2)–Co(1)–S(1)	73.37(5)	S(2)–Co(1)–S(1)	84.60(6)	N(3)–Co(1)–S(2)	111.17(14)
N(8)–Co(1)–S(1′)	171.20(11)	S(2)–Co(1)–S(2′)	84.87(6)	S(1)–Co(1)–S(2′)	157.35(6)
S(1)–Co(1)–S(1′)	84.15(4)				

Table 4
Room temperature magnetic moments and molar conductivity data

Complex	Magnetic moment per nucleus (B.M.)	Molar conductivity (Ω^{-1} cm^2 mol^{-1})
1	5.85	90 (1:1)
3	5.95	77 (1:1)
4	4.70	285 (1:4)
5	diamagnetic	148 (1:2)
6	diamagnetic	8 (non-electrolyte)

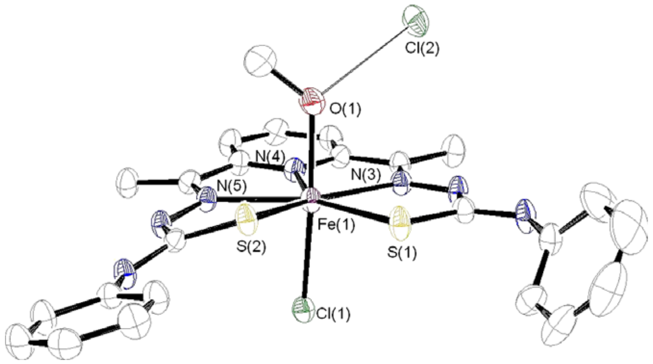

Fig. 4. ORTEP drawing of **2**, showing 50% ellipsoids. H atoms omitted for clarity. The thin line between Cl(2) and O(1) indicates the hydrogen bonding interaction.

bonds (1.668 and 1.676 Å) are again consistent with a neutral ligand with a C–S double bond. Once again, the ligand in **2** is very planar, with dihedral angles involving the planes described above of 10.8° and 3.06°.

A seemingly trivial change involving a switch from $FeCl_3$ to $Fe(ClO_4)_3$ resulted in a surprising result. The only complex that could be isolated was found to be one in which the ligand had been partially hydrolyzed. There is precedence for the hydrolysis of one side of a 2,6-pyridinebis(imine) ligand [16]. Magnetic susceptibility and conductivity measurements are consistent with an $S = 5/2$ species and a 1:1 electrolyte. An ORTEP drawing of the cation in $[(L^{2'})_2Fe]ClO_4$ (**3**) is shown in Fig. 5, with data collection and structure solution parameters in Table 1 and selected bond distances and angles in Tables 2 and 3. The complex sits on a twofold axis in the monoclinic space group $P2/c$ and crystallizes with two molecules of DMF, one of which is disordered. Each ligand maintains the intact thiosemicarbazone on one side of the pyridine ring, but has been hydrolyzed on the other side to reform the ketone functionality. The ligand acts in a tridentate manner with coordination through the pyridine and azomethine N atoms and the S atom. Two ligands complete the octahedral coordination environment of the Fe(III) complex. Fe–S (2.203 Å) and C–S (1.751 Å) bonds in this case are consistent with a monodeprotonated ligand. The ordered DMF molecule forms a hydrogen bond with an N–H group on the Fe complex. Infrared spectra clearly show stretches for both the imine ($\nu_{CN} = 1598$ cm^{-1}) and ketone ($\nu_{CO} = 1713$ cm^{-1}) functionalities, confirming the ligand hydrolysis.

3.2. Cobalt chemistry

While the iron chemistry of these ligands leads to the isolation of mononuclear species, the chemistry with cobalt is dominated by dinuclear species. Two different dinuclear species were isolated depending, once again, on the particulars of the ligand substituents and the cobalt salt.

Using the unsubstituted ligand in combination with $Co(ClO_4)_2$, the Co(II) complex $\{[H_2L^1Co(CH_3CN)]_2\}(ClO_4)_4$ (**4**) is isolated. Magnetic susceptibility measurements are consistent with previous reports of significant orbital contributions to high-spin Co(II) complexes, which yield magnetic moments in the 4.7–5.2 B.M. range [17]. Conductivity measurements are consistent with a 1:4 electrolyte. An ORTEP drawing of the cation in **4** is shown in Fig 6, with data collection and structure solution parameters in Table 1 and selected bond distances and angles in Tables 2 and 3. The dimeric molecule displays structure type **V**, and is situated on an inversion center in the triclinic space group $P\bar{1}$. Each Co atom in **4** is in a pentagonal bipyramidal coordination geometry, similar to the Fe atom in **1**, with the pentadentate ligand occupying the equatorial pentagonal plane. One axial position is occupied by an CH_3CN ligand, while the second axial position is filled by a sulfur atom from the centrosymmetrically related ligand. Until recently, this structural type had not been reported for a complex of a bis(thiosemicarbazone) ligand, but Souza and coworkers reported a similar Zn complex in 2005.[12a] Unlike the Zn dimer, **4** exhibits a symmetric Co_2S_2 core, with bond lengths between Co and the two

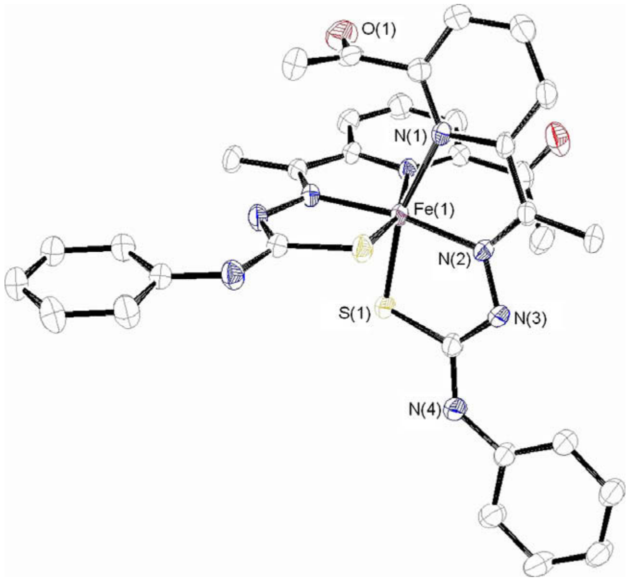

Fig. 5. ORTEP drawing of the cation in **3**, showing 50% ellipsoids. H atoms omitted for clarity.

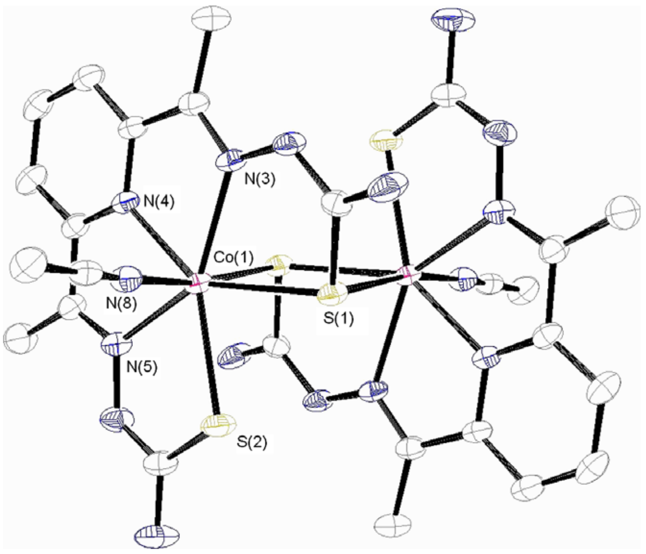

Fig. 6. ORTEP drawing of the cation in **4**, showing 50% ellipsoids. H atoms omitted for clarity.

bridging sulfur atoms of 2.604 and 2.605 Å. Bond lengths to the non-bridging sulfur atom are shorter (2.526 Å), as expected. These Co–S bond lengths and the C–S bond lengths (1.676 and 1.708 Å) are consistent with a C–S double bond and a neutral ligand. The ligand in **4** is still quite planar, but shows a slight helical twist, with the non-bridging thiolate situated 0.333 Å above the plane defined by the Co and the three coordinated N atoms and the bridging thiolate situated 0.506 Å below this plane, towards the other Co. One perchlorate is ordered, while the other has been modeled with one full occupancy O atom and six partially occupied O sites. The disordered perchlorate forms hydrogen bonds to the Co dimer, producing a chain of dimers.

A second type of dimer is isolated when the phenyl-substituted ligand is treated with $Co(NO_3)_2$. An ORTEP drawing of the cation in the Co(III) complex $[L^2Co]_2(NO_3)_2$ (**5**) is shown in Fig. 7 with data collection and structure solution parameters in Table 1 and selected bond distances and angles in Tables 2 and 3. The dimer is situated on a twofold axis in the monoclinic space group *C*2/*c* and crystallizes with two water molecules per dimer. One water molecule and the nitrate counterion are involved in hydrogen bonds with each other and with the Co dimer. Each Co ion is in a distorted octahedral coordination sphere with the five donor atoms of one dianionic ligand and a S from the symmetrically related ligand providing the ligation. This is the first example of a ligand of this type occupying five positions in an octahedral coordination sphere. In order to form this compound, the normally planar ligand must deviate from planarity to an extent not previously observed. This deviation is manifest in two areas. The first, less drastic deviation, is a slight bending of one side of the ligand from planarity. Thus, if one defines a plane containing Co, the pyridine N atom N(4) and C(8) and C(9), one finds that the coordinated azomethine N atom N(3) is 0.14 Å out of the plane and the carbamate N atom N(2) is 0.61 Å out of the plane. This compares with N(5) and N(6) on the other side of the ligand, both of which are only 0.04 Å out of the analogous plane. The second deviation is much more severe – a rotation about the N(2)–N(3) bond such that the torsional angle C(8)–N(3)–N(2)–C(7) is 54° (compared with 6° on the other arm of the ligand). The result is that the carbamate portion on one side of the ligand is almost perpendicular to the rest of the ligand. Using the interplanar dihedral angle measurement defined earlier, **5** shows, *by far*, the largest such angle, 72.48°, of any reported structure involving this class of ligand, especially in those complexes where all five donor atoms are coordinated to the same metal. The resulting coordination geometry still deviates significantly from octahedral symmetry, most notably in that the non-bridging thiolate is tilted towards the open end of the ligand, such that the “trans” S(1)–Co(1)–S(2′) angle is only 157°. The geometry of the Co_2S_2 core is more asymmetric than that in **4**, with a bond length of 2.226 Å to the thiolate from the same ligand (Co(1)–S(2)) and 2.300 Å to the thiolate from the opposing ligand (Co(1)–S(2′)). The difficulty with which this ligand wraps around an octahedral geometry is further manifest in the relatively long bond distance between Co and the terminal thiolate (Co(1)–S(1) 2.292 Å. All of the Co–S and C–S bond distances, however, are consistent with the ligand being in the deprotonated form.

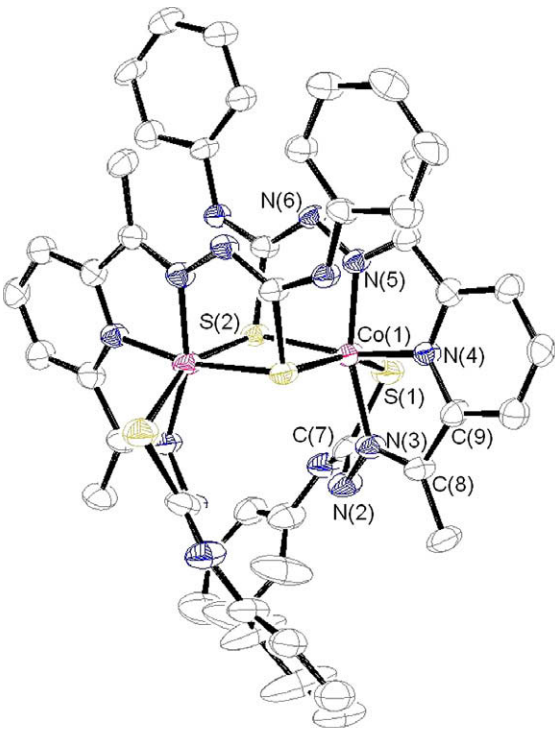

Fig. 7. ORTEP drawing of the cation in **5**, showing 50% ellipsoids. H atoms omitted for clarity.

Compound **5** thus represents a new structural type for this class of ligands. It is similar to three other dimeric species which have been synthesized as precursors to models for the active site of cobalt-containing nitrile hydratase. Mascharak and coworkers have published the synthesis and characterization of $[CoPyPS]_2^{2-}$ with a tetraanionic pentadentate N_3S_2 ligand utilizing one pyridine and two amide nitrogen donors and two thiolate sulfur donors [18]. We have synthesized $[Co(tsaltp)]_2^{2+}$ and a related dimer, both with N_2S_3 ligands containing two imine nitrogen donors, two thiolate sulfur donors, and one thioether sulfur donor [5b,19]. The geometry of **5** is very similar to that of $[CoPyPS]_2^{2-}$ with the three backbone donor atoms (pyridine N and two amide or azomethine N) spanning the meridian of the octahedral coordination sphere, one thiolate S occupying an axial site and the other thiolate S in the same plane of the backbone donors and bridging to the other Co atom. $[Co(tsaltp)]_2^{2+}$ differs in that the backbone donors (one thioether S and two imine N) occupy one trigonal face.

The two Co dimers, **4** and **5**, show very different electrochemical responses. The pentagonal bipyramidal dimer **4** has a pseudo-reversible couple at −475 mV versus Ag/AgCl, likely corresponding to a $Co^{III/II}$ couple and an irreversible couple at −1440 mV, which is in the range that has been seen for $Co^{II/I}$ couples in related complexes [20]. The pseudo-octahedral dimer **5**, on the other hand, shows only an irreversible $Co^{III/II}$ couple at ca. −800 mV. This behavior is very similar to that in $[Co(tsaltp)]_2^{2+}$, which is also a pseudo-octahedral dimer and has an irreversible electrochemical response at ca. −800 mV.

It has been shown that both $[Co(tsaltp)]_2^{2+}$ and $[Co(PyPS)]_2^{2-}$ can be cleaved by addition of cyanide ion to give mononuclear species of the form [LCoCN] (neutral species for $tsaltp^{2-}$ complex and dianion for $PyPS^{4-}$ complex). $[Co(PyPS)CN]^{2-}$ has been further shown to be able to catalyze the hydrolysis of acetonitrile to acetamide,[18] while [Co(tsaltp)CN] has not yet been shown to serve this function at pH < 12. Treatment of **5** with KCN results in the isolation of **6**, which, although not yet structurally characterized, displays a CN stretch in the infrared spectrum at 2122 cm^{-1} and analyzes satisfactorily for $[L^2CoCN]$. With four such species now in hand with different donor sets, it is possible to more thoroughly investigate the geometric and electronic features which bear on the ability of a Co(III) species to catalyze the controlled hydrolysis of the nitrile bond.

4. Conclusions

New iron and cobalt complexes of bis(thiosemicarbazone) ligands have been synthesized and characterized. Complex **3** shows an unexpected hydrolysis of the ligand, while complex **5** displays an unprecedented amount of deviation from planarity, enabling the ligand, for the first time, to occupy five sites of a distorted octahedral coordination sphere. Complex **6** adds to the growing number of octahedral Co(III) complexes with mixed N/S coordination geometries that are being synthesized as model complexes for the active site of Co nitrile hydratase. Further studies are being carried out to characterize the reactivity of this and related species.

Acknowledgement

This work was supported by NIH COBRE Award P20 RR017708 from the National Center for Research Resources (D.M.E.). We thank Dr. Colin Thomas for assistance in checking the synthetic procedures.

Appendix A. Supplementary data

Supplementary data associated with this article can be found, in the online version, at doi:10.1016/j.ica.2008.06.031.

References

[1] E.J. Blanz, F.A. French, Cancer Res. 28 (1968) 2419.
[2] (a) S.P. Mittal, S.K. Sharma, R.V. Singh, J.P. Tandon, Curr. Sci. 50 (1981) 483;
(b) E. Bermejo, R. Carballo, A. Castiñeiras, R. Dominguez, A.E. Liberta, C. Maichle-Mössmer, M.M. Salberg, D.X. West, Eur. J. Inorg. Chem. 965 (1999).
[3] (a) A.S. Dobeck, D.L. Klayman, E.J. Dickson, J.P. Scovill, E.C. Tramont, Antimicrob. Agents Chemother. 18 (1980) 27;
(b) N.C. Kasuga, K. Sekino, C. Koumo, N. Shimada, M. Ishikawa, K. Nomiya, J. Inorg. Biochem. 84 (2001) 55.
[4] J.C. Logan, M.P. Fox, J.H. Morgan, C.J. Pfau, J. Gen. Virol. 28 (1975) 271.
[5] (a) D.M. Eichhorn, N. Goswami, Comm. Inorg. Chem. 24 (2003) 1–13;
(b) B.W. Smucker, M.J. Van Stipdonk, D.M. Eichhorn, J. Inorg. Biochem. 101 (2007) 1537–1542.
[6] (a) T. Nagasawa, H. Nanba, K. Ryuno, K. Takeuchi, H. Yamada, Eur. J. Biochem. 162 (1987) 691;
(b) M. Odaka, T. Noguchi, S. Nagashima, M. Yohda, S. Yabuki, M. Hoshino, Y. Inoue, I. Endo, Biochem. Biophys. Res. Commun. 221 (1996) 146;
(c) M. Odaka, K. Fujii, M. Hoshino, T. Noguchi, M. Tsujimura, S. Nagashima, M. Yohda, T. Nagamune, Y. Inoue, I. Endo, J. Am. Chem. Soc. 119 (1997) 3785;
(d) T. Nagasawa, K. Ryuno, H. Yamada, Biochem. Biophys. Res. Commun. 139 (1986) 1305;
(e) M.J. Nelson, J. Jin, I.M. Turner, G. Grove, R.C. Scarrow, B.A. Brennan, L. Que, J. Am. Chem. Soc. 113 (1991) 7072;
(f) T. Nagasawa, K. Takeuchi, H. Yamada, Biochem. Biophys. Res. Commun. 155 (1988) 1008;
(g) T. Nagasawa, K. Takeuchi, H. Yamada, Eur. J. Biochem. 196 (1991) 581;
(h) B.A. Brennan, G. Alma, M.J. Nelson, L.T. Durney, R.C. Scarrow, J. Am. Chem. Soc. 118 (1996) 9194;
(i) M.S. Payne, S. Wu, R.D. Fallon, G. Tudor, B. Stieglitz, I.M. Turner, M.J. Nelson, Biochemistry 36 (1997) 5447;
(j) A. Miyanaga, S. Fushinobu, K. Ito, T. Wakagi, Biochem. Biophys. Res. Commun. 288 (2001) 1169.
[7] (a) S.W. Ragsdale, M. Kumar, Chem. Rev. 96 (1996) 2515;
(b) S.W. Ragsdale, L.G. Ljungdahl, D.V. DerVartanian, Biochem. Biophys. Res. Commun. 115 (1983) 658;
(c) S.W. Ragsdale, L.G. Ljungdahl, D.V. DerVartanian, Biochem. Biophys. Res. Commun. 108 (1982) 658;
(d) P.A. Lindahl, E. Munck, S.W. Ragsdale, J. Biol. Chem. 265 (1990) 3873;
(e) C.M. Gorst, S.W. Ragsdale, J. Biol. Chem. 266 (1991) 20687;
(f) C. Fan, C.M. Gorst, S.W. Ragsdale, B.M. Hoffman, Biochemistry 30 (1991) 431;
(g) S.P. Cramer, M.K. Eidsness, W.H. Pan, T.A. Morton, S.W. Ragsdale, D.V. DerVartanian, L.G. Ljungdahl, R.A. Scott, Inorg. Chem. 26 (1987) 2477;
(h) J. Xia, J. Dong, S. Wang, R.A. Scott, P.A. Lindahl, J. Am. Chem. Soc. 117 (1995) 7065;
(i) C.Y. Ralston, H. Wang, S.W. Ragsdale, M. Kumar, N.J. Spangler, P.W. Ludden, W. Gu, R.M. Jones, D.S. Patil, S.P. Cramer, J. Am. Chem. Soc. 122 (2000) 10553;
(j) D. Qiu, M. Kumar, S.W. Ragsdale, T.G. Spiro, Science 264 (1994) 817;
(k) M. Kumar, D. Qiu, T.G. Spiro, S.W. Ragsdale, Science 270 (1995) 628;
(l) T.I. Doukov, T.M. Iverson, J. Seravalli, S.W. Ragsdale, C.L. Drennan, Science 298 (2002) 567;
(m) C. Darnault, A. Volbeda, E.J. Kim, P. Legrand, X. Vernede, P.A. Lindahl, J.C. Fontecilla-Camps, Nat. Struct. Biol. 10 (2003) 271.
[8] Range established by a search of the Cambridge Structural Database: F.H. Allen, Acta Crystallogr., Sect. B 58 (2002) 380–388.
[9] (a) W. Huang, J. Jia, J. Cummings, M. Nelson, G. Schneider, Y. Lindqvist, Structure 5 (1997) 691;
(b) S. Nagashima, M. Nakasako, N. Dohmae, M. Tsujimura, K. Takio, M. Odaka, M. Yohda, N. Kamiya, I. Endo, Nat. Struct. Biol. 5 (1998) 347.
[10] M. Mohan, P. Sharma, M. Kumar, N.K. Jha, Inorg. Chim. Acta 125 (1986) 9.
[11] (a) A. Bino, N. Cohen, Inorg. Chim. Acta 210 (1993) 11;
(b) A.H. Othman, K.-L. Lee, H.-K. Fun, B.-C. Yip, Acta Crystallogr., Sect. C 52 (1996) 602;
(c) G. Dessy, V. Fares, Cryst. Struct. Commun. 10 (1981) 1025;
(d) R. Pedrido, M.R. Bermejo, M.J. Romero, M. Vazquez, A.M. Gonzalez-Noya, M. Maneiro, M.J. Rodriguez, M.I. Fernandez, Dalton Trans. (2005) 572;
(e) C.A. Brown, W. Kaminsky, K.A. Claborn, K.I. Goldberg, D.X. West, J. Braz. Chem. Soc. 13 (2002) 10.
[12] (a) A.I. Matesanz, I. Cuadrado, C. Pastor, P. Souza, Z. Anorg. Allgem. Chem. 631 (2005) 780;
(b) G.F. de Sousa, D.X. West, C.A. Brown, J.K. Swearingen, J. Valdes-Martinez, R.A. Toscano, S. Hernandez-Ortega, M. Homer, A.J. Bortoluzzi, Polyhedron 19 (2000) 841;
(c) M.R. Bermejo, A.M. Gonzalez-Noya, R.M. Pedrido, M.J. Romero, M. Vazquez, Angew. Chem., Int. Ed. Engl. 44 (2005) 4182;
(d) E. Labisbal, A. Castineiras, C.A. Brown, D.X. West, Z. Naturforsch., B 56 (2001) 229;
(e) M.S. Shongwe, H.N.R. Kharousi, H. Adams, M.J. Morris, E. Bill, Inorg. Chem. 45 (2006) 1103.
[13] G.F. DeSousa, V.M. Deflon, E. Niquet, A. Abras, J. Braz. Chem. Soc. 12 (2001) 493.
[14] APEX2 User Manual, Bruker AXS, Inc., Madison, WI, 2006.
[15] G.M. Sheldrick, Institüt für Anorganische Chemie der Universität, Tammanstrasse 4, D-3400 Göttingen, Germany, 1998.
[16] B. Le Gall, F. Conan, J.-M. Kerbaol, M.M. Kubicki, E. Vigier, Y. Le Mest, J.S. Pala, Inorg. Chim. Acta 336 (2002) 87–90.
[17] (a) M. Juric, B. Peric, N. Brnicevic, P. Planini, D. Pajic, Z. Kreso, G. Giester, B. Kaitner, Dalton Trans. (2008) 742;
(b) G. Vuckovic, V. Stanic, S.P. Sovilj, M. Antonijeic-Nikolic, J. Mrozinski, J. Serb. Chem. Soc. 70 (2005) 1121.
[18] J.C. Noveron, M.M. Olmstead, P.K. Mascharak, J. Am. Chem. Soc. 121 (1999) 3553.
[19] C.E. Moore, D.M. Eichhorn, unpublished work.
[20] A.K. Singh, R. Mukherjee, Dalton Trans. (2008) 260.